THE ASTROPHYSICAL JOURNAL, 422:164–175, 1994 February 10

THE SIZE DISTRIBUTION OF INTERSTELLAR DUST PARTICLES AS DETERMINED FROM EXTINCTION

SANG-HEE KIM,[1,2] P. G. MARTIN,[2,3] AND PAUL D. HENDRY[1]
Received 1993 July 15; accepted 1993 August 17

ABSTRACT

Variations in the shape of the interstellar extinction curve from place to place in the Galaxy indicate that the size distribution of interstellar dust particles and/or the compositional mix are also changing. Cardelli, Clayton, & Mathis have shown that the extinction changes can be parameterized using the ratio of total to selective extinction, R_V. We have investigated the character of the underlying changes in the size distribution, and illustrate this with two contrasting cases: the diffuse interstellar medium ($R_V = 3.1$), and a dense cloud region ($R_V = 5.3$).

For this exploratory investigation we adopted spherical bare silicate and bare graphite particles as in the Mathis, Rumpl, & Nordsieck (MRN) modeling. To extract the size distributions of the two components as objectively as possible we used the Maximum Entropy Method which gives the smoothest solution compatible with the χ^2 confidence level on the goodness of fit to the extinction data. Abundance constraints were implemented directly in the method in order that the elements incorporated in the grains did not exceed their cosmically available abundances or contradict depletion data.

With the available wavelength range of the extinction data, from 0.1 to 5 μm, the range over which the derived size distributions are reliable is 0.02 to 1 μm in radius a. Note that there is no direct information from extinction on the *shape* of the distribution for smaller grains (<0.02 μm), but their total mass is reasonably well determined. For the largest sizes (>1 μm), the distribution is also unknown, but the abundance constraints can play an active role in limiting their numbers since large particles tend to contribute a significant fraction of the total interstellar dust mass.

The size distribution found by MRN for the diffuse interstellar medium was a smooth power law out to a sharp cutoff at $a_+ = 0.25$ μm. We confirm the qualitative features of this distribution. However, in order to achieve a good fit to the data at U, B, and V where the extinction curve changes slope and in the ultraviolet, the silicate and graphite size distributions depart significantly (and robustly) from a simple power law. We also show how the size distribution falls off smoothly beyond a_+, perhaps compatible with an exponential cutoff.

It has been known for some time that the mean size of particles appears to increase in a denser environment, and our new results for the case $R_V = 5.3$ now quantify this effect. Compared to the case of diffuse interstellar medium, this size distribution has a significant reduction in the number of intermediate and smaller particles (<0.1 μm) and a more modest increase at larger sizes. The implications for the origin and evolution of the grain size distribution are discussed.

Subject heading: dust, extinction

1. INTRODUCTION

The size distribution of interstellar dust particles is of wide astronomical interest, for example in the detailed interpretation or prediction of extinction, infrared emission, or reflection nebulosity. It is needed to evaluate such astrophysical processes as formation of molecular hydrogen on grain surfaces and photoelectric heating of the interstellar gas. Furthermore, the size distribution is interesting in itself, being intimately connected to the origin and evolution of the grains. Consequently it is not surprising that there have been many studies of the size distribution over the past several decades, both theoretically and observationally oriented (Oort & van de Hulst 1946; Greenberg 1968; Hong & Greenberg 1978; Mathis, Rumpl, & Nordsieck 1977, hereafter MRN; Biermann & Harwit 1980; Mathis 1979; Mathis & Wallenhorst 1981; Mathis & Whiffen 1989).

A widely applied size distribution is the one proposed by MRN, a power law $n(a) \propto a^{-3.5}$ extending from a small to a large size cutoff denoted $a_- = 0.005$ μm and $a_+ = 0.25$ μm, respectively. This was based on fitting the interstellar extinction curve of the diffuse interstellar medium, as observed over the wavelength range 0.11–1 μm, using bare graphite and silicate grains. The basic problem is to determine the numbers of particles in each size interval (a size bin). Since there is potentially a wide range of possible sizes contributing to the extinction, there are many more parameters to determine than available data. MRN used quadratic programing to solve this problem, but the resulting size distribution was very spiky, showing gaps in several size bins, which seems unphysical, as they noted. To remove the gaps, they adopted a set of overlapping bins each starting at size zero. Within each such size bin the size distribution was taken to be uniform, in essence assuming a priori an overall smoothly declining distribution.

To provide a more objective solution, we have adopted the Maximum Entropy Method (MEM) which is ideally suited to this problem as posed, with more unknowns than data; MEM solutions are positive (as required) and are characteristically smooth unless otherwise demanded by the data; a smooth

[1] Department of Astronomy, University of Toronto, Toronto, ON, Canada M5S 1A7.
[2] Visiting Theoretical Astrophysics, Caltech, Pasadena, CA 91125.
[3] Canadian Institute for Theoretical Astrophysics, University of Toronto, Toronto, ON, Canada M5S 1A7.

distribution seems a reasonable expectation for interstellar dust.

Most of the work on the size distribution has been focused on the extinction curve of the diffuse interstellar medium, even though there is evidence that extinction, and thus the size distribution, depends on environment. Mathis & Wallenhorst (1981) and Mathis & Whiffen (1989) did address this issue; their approach was to adopt a power-law form for the size distribution as proposed by MRN, but to adjust the parameters (a_-, a_+, and/or the slope) to fit the data. Not unexpectedly, different parameters were required depending on the extinction curve. Again, we felt that MEM would provide both a more objective solution and, being of less specific form, a better fit. This in turn would lay a more secure basis for understanding how and why the size distribution changes with environment.

This is also an opportune time to revisit the size distribution problem, since there is now available a more extensive data base for the wavelength dependence of many stars from the near-infrared through ultraviolet (roughly speaking, data in the near infrared and ultraviolet help to constrain the numbers of large and small grains, respectively). Furthermore, changes in extinction with environment have been placed on a more systematic basis by Cardelli, Clayton, & Mathis (1989, hereafter CCM), leading to the hope that the corresponding systematic changes in the size distribution might be quantified.

In § 2 we introduce the new approach using MEM and summarize our tests of its reliability. Extinction curves, the dust composition, and abundance constraints are discussed in § 3. The size distributions from extinction for $R_V = 3.1$ and $R_V = 5.3$ are determined in § 4, followed by a discussion of related phenomena, scattering and infrared emission, in § 5. Finally, in § 6, we discuss the size distributions in the context of physical processes affecting grain evolution.

2. FITTING THE EXTINCTION

2.1. *Implementing and Evaluating the Maximum Entropy Method*

The extinction period produced along any line of sight is given by

$$\tau_v = A_v/1.086 = \int dl \int_0^\infty \pi a^2 Q_{e,v}(a) n(a) da$$
$$= \int dl \frac{3}{4\rho} \int_0^\infty \frac{Q_{e,v}(a)}{a} m(a) da \qquad (1)$$
$$\simeq \int dl \frac{3}{4\rho} \sum_i m_i \int_{a_i}^{a_{i+1}} \frac{Q_{e,v}(a)}{a} da .$$

For simplicity this has been written for a single grain composition and for spheres, but the generalization to other shapes and multiple compositions is obvious. Usually, the size distribution has been expressed in terms of $n(a)$, the number of particles per unit volume in the size interval a to $a + da$, but as we shall see there are important technical and astrophysical reasons to prefer $m(a)$, the corresponding differential mass. As in MRN, the integral over size is broken up into discrete ranges or bins, labeled i. Given the optical constants of the chosen grain compositions, one can calculate the extinction efficiency factors $Q_{e,v}(a)$ and compute the integrals for each bin numerically assuming $m(a)$ (or some closely related function) is a constant m_i over that bin. The unknowns m_i are to be determined by fitting the predicted extinction to that observed at a number of different frequencies. The goodness of fit is measured by the usual (weighted) χ^2.

In the fitting process within MEM the smoothest possible solution near some prescribed default and consistent within some target χ^2 is obtained by maximizing the Shannon-Jaynes form of entropy (Skilling 1981). In practice the entropy is written:

$$S_M = \sum_i w_i f_i [1 - \ln (f_i/d_i)] \qquad (2)$$

Here f_i is the discretized function to be obtained. The default (or template) d_i is some smooth function containing minimal information about the desired solution. The w_i are simply weights.

Constraints were applied to the total mass of each material so as not to use more than the cosmically available abundances; this requires knowing the amount of extinction per unit hydrogen column density, A_v/N_H (see § 3.3).

The particular MEM implementation used is described by Hendry (1994). The principles behind its operation are essentially similar to those described by Skilling (1981), except that a much improved control procedure was devised, making the algorithm converge several times faster and converge more reliably and precisely, especially in difficult cases, and that the provision for additional constraints (besides entropy and χ^2) was added to the algorithm. Since this is a new application of MEM we have investigated the sensitivity of the solution to various choices that have to be made in practice. The tests were basically to see how well a known size distribution could be extracted from simulated data generated using that size distribution using, e.g., the prescription in equation (1). In practice it is advantageous in MEM to remove any overall slope in the function f sought; for example, if $n(a) \propto a^{-3.5}$ then a much flatter function of a is $m(a) \propto a^{-0.5}$. Our testing of such steep cases indicated that attempting solutions based on $n(a)$ was indeed problematical, but that using $m(a)$ or using the surface area [$s(a) \propto a^{-1.5}$] were equally satisfactory. Consequently the final results we present (§ 4) were determined using the m_i formulation of equation (1). In other simulations we adopted various forms for $s(a)$: a step function, a power law, or a power law with exponential decay (PED) above some size a_b

$$s(a) = s_0 a^{-\gamma} \exp(-a/a_b) . \qquad (3)$$

The size bins were chosen carefully to have a good resolution throughout the entire size range to be explored, $0.0025 < a < 10$ μm. Tests indicated that a logarithmic distribution was satisfactory. Normally we adopted $a_1 = 0.0025$ μm and 60 size bins (scale factor 1.148). Tests of step function simulations show that sharp changes in the size distribution can be recovered.

Because the contribution to extinction at a given bin is linearly proportional to the adopted bin size, w_i was taken to be proportional to the width of the size interval. This is preferred to adopting a constant value, though the latter gave about the same result; the main difference is at the large size end where for constant weight the size distribution becomes relatively more constrained by abundance: the size distribution suddenly drops at ~ 0.7 μm for both silicate and graphite.

Another issue is sensitivity of the extracted solution to the shape of the default d_i [examples used were like those for $s(a)$], or to the shape of the initial guess at the size distribution (same choices). We made test runs with many possible combinations

of the size distribution, a default, and an initial size distribution. In the most basic test, we verified that if a default and a model size distribution have the same shape, then the MEM solution gives a perfect reconstruction throughout the whole size range. The solutions were also independent of initial conditions for all the combinations.

There is, of course, not infinite dynamic range: trace components in the size distribution may produce small changes in the extinction, and vice versa, and so are eventually masked either by errors in the data or in the discretized reconstruction. One representative nonflat size distribution would be a Gaussian; tests indicate that information more than 2 decades below the peak is lost. For a step size distribution, MEM can give a good reconstruction even for a step width as small as one bin and a step height as large as 4 decades. Another pertinent test relates to models with two compositions each with a separate size distribution (more independent parameters to determine); while the astronomical data indicate comparable amounts of silicate and carbon grains, our tests showed that ratios of 10:1 or 1:10 could still be recovered from simulated data.

In MEM the solution f_i will track the shape of the default d_i unless there is some information in the data that warrants a change. Because there is a finite frequency range spanned by the data, one would expect that there would also be a finite size range $(a_l - a_u)$ for which the solution would be objective: within this size range, the solution is independent of the default; outside of it the solution follows the shape of the default. Our tests (for a two-composition model such as will be studied) indicate that this size range is ~ 0.02–1 μm for the adopted range of data, 0.1–5 μm.

The reason for the lower cutoff in information on the size distribution, at $a_l \simeq 0.02$ μm is not that smaller particles cease to contribute to the (far-ultraviolet) extinction. Rather for these particles the size parameter $x = 2\pi a/\lambda$ is considerably smaller than unity over the frequency range examined, and so the extinction is predominantly from absorption for which $Q_{e,v}(a)/a$ is a constant with a. Because these smaller particles extinguish per unit mass, there is no information from extinction regarding the *shape* of their mass distribution. The MEM solution therefore follows the default below a_l. The total mass in size bins below a_l is almost independent of the default (as expected: see eq. [1]), but even this is not without complications. In fitting the far-ultraviolet data there can be some tradeoff between large-particle (neutral) and small-particle (wavelength-dependent) contributions, and between particles of different compositions, depending on the shape of a default.

Grains larger than a_u, by contrast, have an appreciable size parameter over most of the frequency range, and so for these the extinction tends to be featureless or gray; again different larger sizes are indistinguishable. The MEM solution again follows the default, or equally diagnostic, produces a ragged distribution. The solution implies a constraint on total surface area of these larger particles. However, since larger particles have higher ratios of mass to surface area, this can lead to an excessive amount of material in these grains, depending on the default being followed, and difficulty obtaining a smooth MEM solution. If there is a tighter constraint on mass from cosmic abundances, then this can suggest an appropriate form for the default in the region $a > a_u$. Nevertheless, it is important to note that by fitting extinction data to wavelengths as long as $\lambda = 5$ μm, we are able to obtain unambiguous information on the important falloff of the size distribution over the range $a = 0.2$–1 μm; if as in MRN we used information only to $\lambda = 1$ μm, then we lose information beyond $a_u = 0.3$ μm, near a_+ where the MRN power law is truncated (see Fig. 1*a*).

2.2. *Independent Checks on Our Final Results*

As one check of the basic features of the MEM solution for the diffuse interstellar medium, we have the original MRN size distribution derived by an independent numerical method. As will be seen in § 4.1, this comparison is favorable.

Our derived size distributions appear to be roughly power laws, with a smooth cutoff toward larger sizes. This suggests an alternative check. Suppose the size distribution is of some functional form, in this particular case PED (eq. [3]). There are three parameters, m_0, and a_b, to be determined for each composition (the smallest size a_- was set to 0.0025 μm). This problem can be solved by nonlinear least squares to find the best fit to the extinction curve. The basic iteration is straightforward, although in computational cost nontrivial: for any given set of values of the parameters, whether the initial guess or subsequent improvements, the predicted extinction at each frequency has to be computed and then χ^2 evaluated. The parameter iteration was carried out by the downhill simplex method to minimize χ^2. Using PED size distributions with six unknowns (three for silicate and three for graphite) provides a lot of flexibility in the potential solution and yet we found size distributions with the same characteristics as those from MEM (§ 4.1): slope, position of the cutoff, and ratio of silicate to graphite. With MEM, of course, the solution is not bound to be any particular form, and so the solution can acquire more structure in conjunction with reaching a lower χ^2.

3. OBSERVATIONAL CONSTRAINTS ON THE SIZE DISTRIBUTION

3.1. *Parameterized Extinction Curves*

The size distribution of interstellar dust particles is to be determined by fitting the wavelength dependence of the extinction of starlight. In their analysis of extinction curves for lines of sight probing different environments, CCM found that the extinction curve over the wavelength range $0.1 < \lambda < 3.3$ μm could be written in analytical form which depends on only one parameter, the ratio of total to selective extinction, $R_V = A(V)/E(B-V)$; R_V is therefore a diagnostic of how the whole curve changes from the diffuse interstellar medium ($R_V = 3.1$) to what is often found in more dense clouds (we shall use $R_V = 5.3$ as a representative example).

Instead of fitting the data for particular stars, we used the typical curve from the CCM formula giving information from the near infrared to vacuum ultraviolet. The sampling ("data") can be seen in the figures below: uniform in wavenumber from 1 to 10 μm^{-1} and fairly uniform in wavelength over the range 1–5.1 μm. In the infrared, the CCM formula is a power law of index 1.61. More recently, Martin & Whittet (1990) showed that a power-law form might extend as far as 10 μm, with index ~ 1.8. The derived size distribution is not very sensitive to the uncertainty in the power-law index.

In their analysis CCM also showed the scatter of the observed data for individual lines of sight around their average formula. This standard deviation is greater in the ultraviolet, reflecting the wider cosmic variation there rather than measurement uncertainty for particular lines of sight; the scatter has been discussed by Cardelli & Clayton (1991) and by Mathis & Cardelli (1992). Therefore, the uncertainties σ in the extinction, used in χ^2, were set to be 1% uniformly at each frequency. We did not find it necessary to choose artificially

smaller values of σ near 2200 Å in order to fit the extinction bump, as MRN did.

Some other observational constraints, not used directly here, are discussed in § 5.

3.2. *Composition*

Any determination of the size distribution presupposes some knowledge of the component materials. For simplicity we adopt the same two as MRN: silicate and graphite. We used the optical constants determined by Draine & Lee (1984; see also Draine 1985). It was assumed that the grains were homogeneous spheres; for graphite, an anisotropic material, extinction was determined by the usual $\frac{1}{3}$–$\frac{2}{3}$ approximation (see, e.g., Draine 1988). Anything inappropriate about any of these assumptions will be propagated to some extent into the derived size distribution. We are more concerned about the evolution of the size distribution. Evaluation of *differential* changes of the size distribution with environment should be less sensitive to these choices than the size distributions themselves. However, it might be that the basic materials to be considered change significantly with environment.

Various forms of carbon-dominated grains have been suggested as the carrier of 2200 Å extinction bump. Small graphite particles still seem to be a promising form (e.g., Draine 1988; Mathis 1994). There is no such specific evidence that carbon in larger particles is in the form of graphite. Therefore, in order to investigate the sensitivity of the size distribution to this choice we have considered some three component models incorporating amorphous carbon (§ 4.1.1). We used optical constants BE1 from Rouleau & Martin (1990).

3.3. *Abundance Constraints: Dust-to-Gas Ratio*

To evaluate masses and incorporate abundance constraints we adopt densities 3.3, 2.26, and 1.81 g cm^{-3} for silicate, graphite, and amorphous carbon, respectively, and a mean molecular weight of 170 per Si in the silicate. In the MRN model (Draine & Lee 1984), silicates use Si/H = 3.2×10^{-5} or 90% of the cosmically available Si (3.55×10^{-5}; Grevesse & Anders 1989) and similar amounts of Mg and Fe, consistent with depletion studies in the diffuse interstellar medium. This illustrates the real potential for using more Si than is available, and so an abundance constraint is incorporated, to be used actively within MEM if required. The depletion situation for C is less clear for several reasons: the undepleted cosmic abundance ratio of C to H is more uncertain, ranging from 3.63×10^{-4} (Grevesse & Anders 1989) to 4.87×10^{-4} (Meyer 1988); gas phase column densities of C have been more difficult to measure; and f values for the measured lines are uncertain. Recent analysis of three stars (Cardelli et al. 1993) show gas phase C II/H = 1.3–2.5×10^{-4}. For comparison, for the graphite grains in the MRN model C/H is 3×10^{-4}, which is appreciable on any scale. With the silicate abundance constrained, for the diffuse interstellar medium we get the same C/H abundance as MRN without a rigid constraint.

To use these constraints, it is necessary to know the normalized form of extinction, $A_v/N_{\rm H}$. For the diffuse interstellar medium, the ratio $E(B-V)/N_{\rm H}$ is fairly well measured (Bohlin, Savage, & Drake 1978); combining this with $R_V = 3.1$ we have

$$A_V/N_{\rm H} = 0.53 \times 10^{-21} \text{ mag cm}^{-2} . \quad (4)$$

The situation for the dense cloud regions is less clear, basically because it is difficult to measure $N_{\rm H}$ or the depletion. What about the dust to gas ratio? If coagulation were the main process affecting the evolution of the size distribution from diffuse to dense clouds (§ 6), then it would be reasonable to adopt a constant mass fraction independent of environment; the ratio of mass in silicate material to mass in carbon material would be constant too (however, unlike our simple model there might be composite grains). Some increase in dust to gas mass ratio might be possible if accretion is effective, but since depletion is already high in the diffuse interstellar medium, the increase must be modest and more probably in the carbon-based materials.

Consequently, for the dense cloud case the size distributions were determined by fitting the shape of the extinction curve, at first without regard to its normalization. Only the relative amount of silicate and carbon grains was constrained to be less than or equal to the diffuse cloud value. Adoption of a ratio of silicate dust to gas that is independent of environment gives a normalization of these size distributions with respect to $N_{\rm H}$; the model computations then give a normalization of $A_v/N_{\rm H}$. This normalization is fairly insensitive to the compositions used; therefore, as a second potential iteration (not necessary here), this normalized extinction curve could be fit incorporating abundance constraints.

4. INTERSTELLAR SIZE DISTRIBUTIONS

4.1. *Diffuse Interstellar Medium: $R_V = 3.1$*

The size distributions for the diffuse interstellar medium derived for silicate and graphite components are displayed in Figure 1a. Also plotted for comparison are the MRN power laws. In this representation we plot $m(a)a$ (dimension mass) normalized to the mass of hydrogen in the same volume so that contributions to the total mass from equal logarithmic intervals in a (or m) can be seen by inspection (see also Fig. 5 of Désert, Boulanger, & Puget 1990). The total dust to H mass ratio is 0.0057 and 0.0035 for silicate and graphite components, respectively.

To a first approximation our MEM size distributions resemble power laws with an exponential cutoff; the overall power-law slope found by MRN is roughly reproduced. Therefore, as described in § 2.2, we fitted parameterized PED size distributions to the extinction data for an independent check of results. These size distributions are also plotted in Figure 1*a*. Despite the overall similarity to MRN, there are nevertheless important differences in the MEM size distributions. We shall discuss intermediate, large, and small sizes in turn.

At intermediate sizes (0.02–0.2 μm), the MEM size distributions have more structure than a simple power law. To clarify the origin of this structure, we display in Figure 1*b* the extinction corresponding to the various size distributions, MRN, PED, and MEM, for comparison with the data. It can be seen that for the smooth power laws in MRN (slope -3.5) or PED (slope -3.06 for silicate and -3.48 for graphite) for intermediate-size grains, the fit to the data in the optical range is not precise. This is reflected in the higher χ^2 for these models (~ 700 for 34 data points for the PED solution). If such a high χ^2 were accepted (set as the target) in the MEM solution, then a similarly poor result is obtained. In the materials used in this model, there is no structure in the frequency dependence of the dielectric function to produce such an effect, and so the size distribution must be altered. Thus the MEM silicate and graphite size distributions for intermediate sizes depart significantly from a simple power-law form. This structure is robust within the context of this graphite-silicate model. For example,

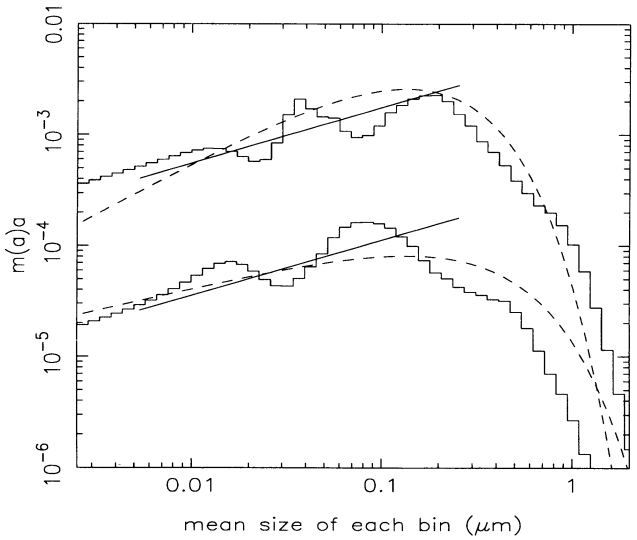

FIG. 1a

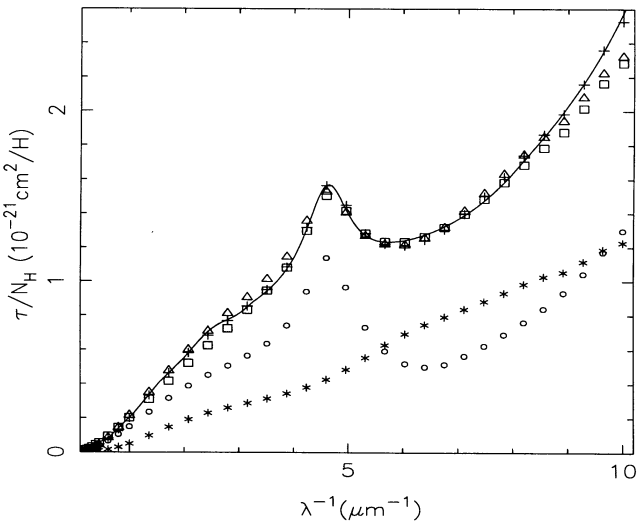

FIG. 1b

FIG. 1.—Diffuse cloud extinction, $R_V = 3.1$. (*a*) The resultant mass distribution, expressed relative to the mass of hydrogen. The upper histogram is for silicate and the lower one is for graphite (scaled down by a factor 10 for clarity). The two solid lines are the corresponding MRN power laws. The two dashed lines are PED size distributions fit to the extinction curve. (*b*) The corresponding extinction curve normalized with respect to hydrogen column density. Crosses are the extinction predicted by the MEM solution at the frequencies fit. Triangles and squares are from the MRN and PED size distributions, respectively. Small circles and asterisks are the MEM contributions of graphite and silicate, respectively. The solid line is the CCM parameterized extinction curve.

even if we start with a broad Gaussian default purposely peaked at the position of the noticeable dip in the silicate size distribution near 0.08 μm, the same dip is recovered. Tests show that the peak at the larger size is related to the shape of the optical extinction. The peak at the smaller size ($\sim$0.03 μm for silicate and $\sim$0.015 μm for graphite) is related to the ultraviolet extinction; in particular, the 2200 Å feature makes specific demands on the graphite component, while the 0.03 μm peak of silicate is necessary to fit the residual ultraviolet extinction that is not explained by the graphite (see Fig. 1*b*). This raises the question of the dependence of this structure on the choice of dielectric function for graphite and on how the extinction for this anisotropic material has been approximated. The effect of changing the basic materials is also explored in the next subsection.

We next turn to the large particle end of the size distribution. It can be seen that the MRN curves are rising with increasing a and that the total mass is kept finite by (presumably artificial) truncation at a_+. Our MEM result shows a smooth decrease beginning at about $\sim$0.2 μm, not surprisingly near a_+, the largest size in the MRN truncated power law. The presence of a decrease out to 1.0 μm is independent of the default adopted: it is forced on the solution by the extinction data. The major contribution to χ^2 in the MRN solution comes from the near infrared; again the MEM solution is more flexible (than simple truncation in this case) and provides a very good fit to the data (although not well appreciated in Fig. 1*b*). The frequency dependence of the infrared extinction has been described by various power-law indices, like -1.6 (CCM) or -1.8 (Martin & Whittet 1990); small changes like this do not produce very different size distributions.

In the PED size distribution, the position of the exponential cutoff is governed by a free parameter a_b; the decrease is found to occur over the same size range as in the MEM solution ($a_b = 0.14$ μm for silicate and $a_b = 0.28$ μm for graphite). The PED size distribution of course extrapolates to larger sizes for which there is no information on the shape of the distribution contained in the extinction. A continued decay of the size distribution is necessary to avoid consuming C and Si in more than their cosmic abundances. Therefore, in the default for the MEM solutions shown an exponental decay was adopted; at the largest sizes the MEM solution more or less follows the shape of this default.

For small grains ($<$0.02 μm), determining the shape of the size distribution is not possible, as discussed in § 2.1. The size distribution is just a replica of the shape of defaults. Since it seemed unlikely that there would be a marked change in the shape of the size distribution just where we were unable to detect it, we adopted a default based on the shape of the derived (real) solution at intermediate sizes (changing the default has no feedback on this region). This results in a size distribution that extrapolates smoothly to the smallest particles (Fig. 1*a*); while cosmetically pleasing, this is only suggestive. The integrated mass for $a < a_l = 0.02$ μm is fairly well constrained by the extinction data for $R_V = 3.1$, independently of the default discussed in § 2.1. For both silicate and graphite components the fraction of the total mass is $\sim\frac{1}{4}$.

The MEM solutions tend to use the maximum amount of Si allowed, fairly independently of the adopted default shape. In Figure 1*a*, 3.37×10^{-5} Si atoms per H or 95% of the adoped cosmic abundance (§ 3.3) is required to be in silicates. The implied depletions of Mg and Fe (which have similar cosmic abundances) in silicate form are high too. The graphite component uses C/H $= 3.0 \times 10^{-4}$. Our estimates of the amount of C and Si in grains are comparable to those of the MRN model (see also Draine & Lee 1984).

4.1.1. *A Three-Component Model*

Like the above MEM solution, most models of interstellar grains incorporate a substantial amount of C. However, the material in which most C is found need not be graphite. In the MEM solution, much of the graphite mass is in intermediate or

large particles which do not produce a 2200 Å extinction bump; but the spectroscopic rationale for incorporating graphite applies to small particles. Therefore we investigated one alternative material, amorphous carbon, again taken to be in the form of homogeneous spherical particles. Because of the 2200 Å feature, a two-component amorphous carbon plus silicate MEM solution does not converge.

We then added a third component, graphite. To minimize the graphite requirement thus making the model as different as possible, we used as a default size distribution a PED with $a_b \simeq 0.02$ μm (a typical small size), and we included size bins for graphite only up to 0.04 μm in order to limit the number of extra parameters to be found. In this three component model, C/H $= 0.81 \times 10^{-4}$ in graphite, $\sim$30% of the total C/H $= 2.73 \times 10^{-4}$ in carbon grains. The role of the larger graphite particles in obtaining a good fit is taken over by the amorphous carbon. The overall size distributions for two- and three-composition models are similar: the MEM solutions for amorphous carbon and silicate are still roughly PED size distributions. It would be interesting to see if the overall size distribution would stay similar for additional different compositional combinations containing C, like graphite plus organic refractories and PAH.

What about the secondary peak structure in the silicate size distribution near 0.03 μm, which was discussed above? We find that now this peak is no longer present; with the added flexibility of a second contributor to the residual ultraviolet extinction smooth size distributions for silicate and amorphous carbon are obtained. The same type of effect occurs in the size distribution solutions for the dense cloud extinction curve. Thus one must be cautious in interpreting any detailed structure found; the MEM size distribution will be a good solution for the adopted building blocks, but the building blocks might not be entirely appropriate.

4.2. *Dense Cloud Extinction with* $R_V = 5.3$

The shape of the extinction curve is substantially different for $R_V = 5.3$ than for $R_V = 3.1$, and so changes in the size distributions are expected. As Cardelli & Clayton (1991) have pointed out, lines of sight with large R_V are ideal for examining processes that modify the grain properties in dense clouds. Although we tend to refer to dense cloud extinction and large R_V interchangeably, we note that not all dense clouds have such large R_V.

Some MEM two-component solutions are shown in Figure 2*a* and the corresponding good fit to the extinction is displayed in Figure 2*b*. Perhaps the most striking change is for intermediate and small sizes: the relative numbers of particles with $a < 0.1$ μm is much reduced for both silicate and graphite components. This quantifies what is needed to understand the flatter behavior of the extinction curve through the ultraviolet. Using a simple power-law prescription, Mathis & Whiffen (1989) found the index was reduced by 1.2 (flattening of the size distribution) in going from $R_V = 3$ to 4.6, which is similar to the effect we find.

The *shape* of the size distribution for $a < 0.02$ μm is again not constrained by the data. But as can be judged directly from Figure 2*a* the fraction of the total mass contained in these small particles has decreased markedly compared to the diffuse cloud case. For silicate the fractional mass has fallen from 0.23 to 0.02; since the proportion of the far-ultraviolet extinction that is wavelength dependent, and to which the small particles respond, is now smaller compared to the "neutral" contribution from larger particles, there is now some sensitivity to the adopted default. Small graphite particles produce the 2200 Å extinction bump which is still prominent, and so the sensitivity of the mass fraction is not great. This spectral requirement also accounts for the obvious structure in the graphite size distribution, which is not as smooth as that for silicates. The fractional mass of graphite in small particles has fallen, however, from 0.25 to 0.09.

Substitution of large amorphous carbon particles in the role of large graphite particles, as in the three-component model for $R_V = 3.1$, was attempted to find an alternative to the derived "bimodal" graphite size distribution. We found that the size distribution for the amorphous carbon component can fall off

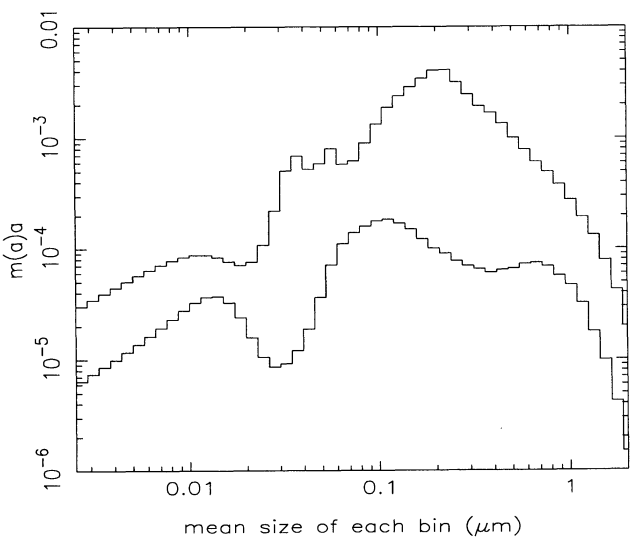

FIG. 2*a*

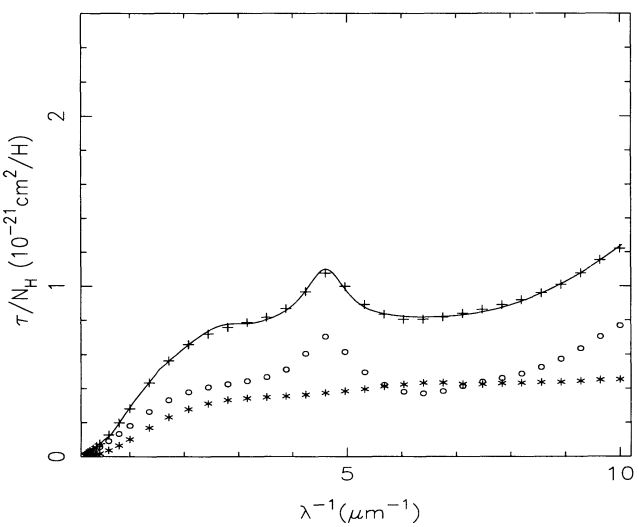

FIG. 2*b*

FIG. 2.—Same as Fig. 1, except for the case of dense cloud extinction, $R_V = 5.3$. (*a*) Mass distribution assuming the silicate to hydrogen mass ratio is the same as for $R_V = 3.1$. (*b*) The corresponding extinction curve.

smoothly toward small sizes like that for silicate. Again, only small graphite particles need be present, now taking a smaller fraction, 0.14, of the total carbon material in grains.

As discussed in § 3.3, in these solutions the mass ratio of silicate to graphite was constrained to be less than or equal to the ratio found for the diffuse cloud; in the solution, the ratio decreased only slightly. Then we renormalized the size distribution (Fig. 2*a*) and the extinction (Fig. 2*b*) so that the total mass of silicate with respect to hydrogen is conserved. Compared to the diffuse cloud, the dense cloud A_V/N_H is 1.2 times larger; Mathis & Whiffen (1989) estimated this increase to be 1.16 (using $R_V = 4.3$). Comparing Figures 2*b* and 1*b* we see that the relative A_v/N_H is increased throughout the infrared (reaching a ratio 1.8) and decreased throughout the ultraviolet.

Since mass in the form of small- and intermediate-sized particles has been removed, there is a corresponding increase for $a > 0.2$ μm. But because the adopted shape of the infrared extinction curve is invariant with R_V, so too is the shape of the derived size distribution between 0.2 and 1.0 μm. Note that the shape of the size distribution for graphite between 0.1 and 1.0 μm is somewhat flatter than that for silicate, just as for $R_V = 3.1$. This is a consequence of the ratio of the silicate and graphite contributions to the infrared extinction being preserved: the detailed shape of the infrared extinction depends on both size distributions for larger particles and on their relative levels.

5. OTHER OBSERVATIONAL CONSTRAINTS

5.1. *Scattering*

From the MEM size distributions we can calculate the scattering properties of the interstellar grains. Two commonly used diagnostics are the albedo, ω (Fig. 3*a*) and the asymmetry parameter of the phase function, g (Fig. 3*b*). For $R_V = 5.3$, both the albedo and g are increased because of the relative shift in importance from smaller to larger particles. In comparisons with data it will therefore be important to take into account the characteristic R_V for the observed region; for example, bright reflection nebulae are more dense than diffuse interstellar clouds and might tend to have higher R_V. Within the frequency range 1.0–10 μm^{-1} the properties for $R_V = 3.1$ are quite similar to those we calculate from the MRN distribution (see also Draine & Lee 1984); in the far-ultraviolet the albedo is somewhat lower because our MEM size distribution is allowed to extend to smaller sizes.

There are significant differences in the infrared (>1 μm), because the MRN power laws are truncated abruptly at $a_+ = 0.25$ μm, while the derived MEM size distributions fall off more smoothly through larger particles. Compared to the MRN model, the scattering is somewhat less isotropic, but the more important difference is in the albedo, which is markedly increased toward lower frequencies (reaching a factor of 6.5 by 5.1 μm).

The albedo and g are not measured directly, but are obtained by modeling observations of scattered light; sometimes only a combination of ω and g is determined. It would be straightforward to use derived values of ω and g actively in the MEM solution of the size distributions. However, as noted by Hurwitz, Bowyer, & Martin (1991), "because of the uncertainty in the observationally determined scattering properties of grains, these parameters have historically not been treated as important constraints on models of dust composition and grain size distribution." Recent observational studies support this point of view. This is not the place for a full critique; instead we will note some of the issues in the context of our model predictions.

Désert, Boulanger, & Puget (1990) compare the albedo of diffuse scattered Galactic light (Lillie & Witt 1976), a high-latitude dust cloud (Laureijs, Mattila, & Schnur 1987), and an H II region (Morgan 1980). The albedos are somewhat discordant; for example in the optical, there is a range up to a factor of 2 between the measurements. We conclude that in our optical our model is acceptable (cf. MRN). In interpreting optical scattering data, the complication of fluorescence in the 1.5 μm^{-1} range (ERE: e.g., Boroson & Witt 1990) should be noted.

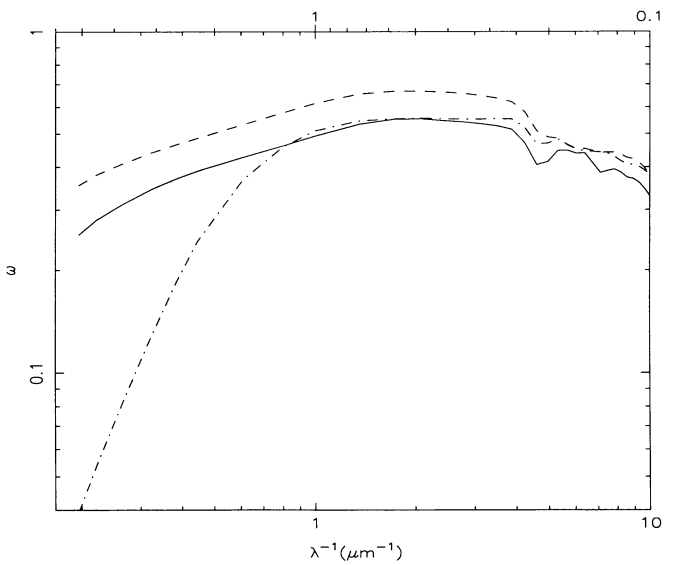

FIG. 3*a*

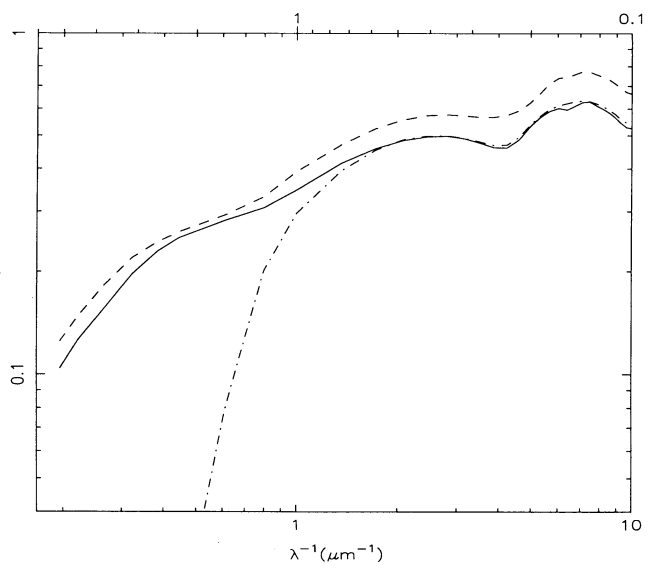

FIG. 3*b*

FIG. 3.—Scattering parameters predicted for different size distributions. (*a*) Albedo (ω); (*b*) asymmetry parameter (g). The solid line is for $R_V = 3.1$ and the dashed line is for $R_V = 5.3$, as calculated from the MEM size distributions. The dash-dotted line is from the MRN size distribution for $R_V = 3.1$.

There are no data on diffuse scattered light in the near-infrared, but there is interesting relevant work on classical reflection nebulae. But there the issue of infrared scattering properties of dust is complicated by nonequilibrium emission by very small grains and/or PAH continuum emission following absorption of a single ultraviolet photon (Sellgren, Werner, & Dinerstein 1992 and references therein), which tends to dominate even at the H and K bands. Linear polarization, a characteristic of the scattered light component, has been used to separate the two contributions. Their models using the Draine & Lee (essentially MRN) albedos tend to predict too little surface brightness, particularly at K. It is interesting, therefore, that the wavelength dependence of the albedo from the MEM size distribution is less steep, working in the direction to correct this exaggerated deficiency at K. The overall albedo is also higher when R_V is, but it seems unlikely that this is a full explanation. For example, Sellgren et al. (1992) show that modelling of NGC 7023 is complicated by a clumpy density distribution. Note also that in the dust model the silicate component has a higher near-infrared albedo than graphite. Therefore, if a carbon bearing material with less infrared absorption than graphite were substituted in the large grains the albedo might be enhanced; candidates to consider are hydrogenated amorphous carbon and organic refractories (e.g., Jenniskens 1993).

In infrared reflection nebulae associated with embedded stars in dense molecular clouds, scattered light is believed to dominate. Pendleton, Tielens, & Werner (1990) have studied the wavelength dependence of the absolute level of the scattered light and its linear polarization. In their modeling they found that the MRN albedo was inadequate: it produced too low a surface brightness, again particularly at the longer wavelengths (out to 5 μm). They explored the effects of larger grains using a shifted simple power law ($a_- = 0.25$ μm, $a_+ = 0.8$ μm), finding them to be beneficial. Likewise, the albedo for the MEM size distribution, particularly that for $R_V = 5.3$ which is likely more relevant to the observed regions, should offer an improvement. We also note that the infrared extinction curve from their shifted size distribution is unlikely to resemble the data characteristic of this region, and so as they appreciated their modification might not be fully consistent. Our size distribution at large sizes, based on an extinction power-law index of -1.6, might be imperfect too. In the Orion molecular cloud there appears to be an extreme power-law index of -1.28 (Martin & Whittet 1990); in such a case, the cutoff in the MEM size distribution would be less steep and the albedo would be even higher.

In the ultraviolet there have been numerous measurements of both classical bright reflection nebulae and the diffuse scattered light in the Galaxy, with rather discordant results (see summary table in Hurwitz et al. 1991). One consistent result seems to be a decrease in albedo at the 2200 Å extinction bump, which is at least qualitatively consistent with the model prediction. Interpretation of recent UIT measurements of NGC 7023 (Witt et al. 1992) have led to radically different values of ω and g compared to earlier observations. Particularly puzzling is the revised high albedo in the far-ultraviolet (~ 1400 Å; $\omega \gtrsim 0.65$). Most materials have sufficient electronic absorption at these high frequencies that when the grains are large enough to scatter efficiently the absorption is also large; therefore, it is difficult to have such a high albedo. The model by Désert et al. (1990), which invokes PAH absorption to cause the far-ultraviolet extinction rise, naturally has a low albedo (0.4) too. The Witt et al. revised value of g is also high (0.7) at 1400 Å, perhaps a little high compared to the models (we suspect that one way to increase g theoretically would be to consider fluffy grains, which have a lower effective refractive index and a larger characteristic size). As mentioned, modeling of NGC 7023 (and perhaps others) is complicated by a clumpy density distribution, and so perhaps the interpretation is still subject to change.

Results by Onaka & Kodaira (1992) on high-latitude diffuse scattered light around 1500 Å are more in accord with the MEM model, having a lower ω and more moderate g. However, they note that Hurwitz et al. have reached a different conclusion, advocating a low albedo (0.2) and quite isotropic scattering; the origin of the difference appears to be inclusion of low-latitude data in the analysis by Hurwitz et al. (e.g., their Fig. 4). Hurwitz et al. show that lowering both ω and g theoretically is difficult, but perhaps not impossible. Again we feel it more likely that the modeling, here of the low-latitude data, might need to be made even more sophisticated.

Grains absorb radiation in the ultraviolet and emit this energy in the infrared. Therefore an important theme that appears is the connection between the ultraviolet albedo and the level of infrared emission.

5.2. *Infrared Emission*

In fact, the predicted brightness of the thermal emission from the MRN model (Draine & Lee 1984) is close to that of the infrared cirrus detected by *IRAS* at 100 μm (Draine & Anderson 1985). At longer wavelengths, the predicted brightness falls off, depending on the adopted dielectric functions, and for some materials possibly on the grain shape and topology. For the same materials, and for spheres as in MRN, the MEM size distributions produce the same thermal emission.

The measured *IRAS* brightness at the other passbands (60, 25, and 12 μm) is systematically above the thermal prediction from these size distributions, growing as the wavelength decreases. Draine & Anderson (1985) interpreted this as the effect of nonequilibrium emission from small grains. Using the MRN size distribution, incorporation of nonequilibrium emission helps to account for the 60 μm brightness, but the model still falls short at 25 and 12 μm. Therefore, they extended the MRN size distribution to include even smaller grains, which spike to higher temperatures. By using both a steeper power-law index and lowering a_- by a decade to 0.0003 μm (3 Å), they achieved an improved fit to the *IRAS* data. We have commented that the shape of the size distribution is not constrained for these very small sizes, but that the total mass is. The extended size distribution has more mass in the small particle range, and we verified that it produces too much extinction in the ultraviolet. One way to obtain consistency with both *IRAS* and the ultraviolet extinction might be to remove some small particles (~ 0.01 μm), although this seems artificial.

A significant fraction of the observed power radiated by dust is at the shorter wavelengths, and so this is an important issue to resolve. The Draine & Anderson model is not the only attempt. For example, Désert et al. (1990) have developed a detailed multicomponent model addressing both the extinction and the infrared emission. Their model includes intermediate-sized grains, carbon-dominated very small grains, and a collection of PAH molecules, each component with a power-law size distribution. PAH is an interesting new component which could contribute both line and continuum emission in the

short-wavelength *IRAS* bands. Although the properties of proposed PAH molecules and their ions are not fully understood, it seems that they might convert ultraviolet and optical photons into the shorter wavelength emission more efficiently (per unit mass), having less of an impact on the extinction curve. Note also that in terms of mass fraction, the PAHs in this model are not a simple extension of the grain size distribution.

In our $R_V = 5.3$ results, applicable more to dark molecular clouds, small particles are systematically removed which would lower the 60/100 μm ratio. If very small particles and/or PAH molecules were removed as well, then the nonequilibrium emission at 12 and 25 μm would also be very much reduced. Observational support along these lines is given by Boulanger et al. (1989) and Sellgren, Luan, & Werner (1990). Désert et al. (1990) take an alternative approach, exploring what changes in the extinction curve are implied by the observed changes in infrared colors. In other regions the influence of strong radiation fields (in photodissociation regions/reflection nebulae and H II regions) on the relative abundances of the small grains and PAHs has to be considered too.

The MEM size distribution for silicate shown in Figure 1*a* has been extended to 0.0025 μm; however, as we noted above, from the extinction alone we do not know more than the total mass of silicate material integrated over $a < a_l = 0.02$ μm. But it can be noted that even smaller silicate grains ($a < 0.001$ μm) would produce nonequilibrium emission at mid-infrared wavelengths, and since silicate has a strong resonance near 10 μm, this feature would appear in the infrared emission spectrum (see Draine & Anderson 1985, then Fig. 2). This is not detected in classical reflection nebulae or in the starburst galaxy M82 (Sellgren et al. 1985; Désert et al. 1986; Siebenmorgen, Krügel, & Mathis 1992), and so the silicate size distribution should certainly not be extended any further than we have shown.

We conclude with a cautionary note about multicomponent models, motivated in particular by the above discussion. Roughly speaking, the grains whose specific signature can be detected in extinction do not produce nonequilibrium emission—a separate component has to be proposed; conversely, this very small grain component is not easily distinguished in extinction alone, nor can it account for all of the extinction—a separate larger component has to be proposed. More generally, a multicomponent model concocted to explain many specific independent phenomena (Rowan-Robinson 1992; Désert et al. 1990) can be comprehensive, but if each component does not by itself explain two or more phenomena, then the model is not necessarily unifying or particularly unique.

6. DISCUSSION

Newly formed grains are injected into the interstellar medium by AGB stars and probably supernovae. The injected size distribution must have some influence on the end product, on both the materials found and the shape of the size distribution. However, the timescale for material to cycle from the diffuse medium to molecular clouds and back is at least an order of magnitude shorter than the injection timescale, and so there is the potential for in situ alteration of the size distribution if growth and destruction processes are sufficiently efficient.

Empirical demonstration of the efficiency with which the grain size distribution is altered *even within one cycle* is found in the very different size distributions derived above for diffuse and dense cloud regions. How this dependence on environment can be interpreted in terms of evolutionary processes is discussed briefly here. Much of the work on interstellar extinction, and on the interstellar medium in general, has been on the diffuse cloud component which historically has been more accessible to optical and ultraviolet examination. Therefore, there might be some tendency to regard the size distribution in the diffuse cloud medium as the "normal" one, and to consider the evolution of the size distribution only as the medium transforms from diffuse into molecular cloud state. This singular view should be resisted since it embraces only half of the story. At the solar Galactocentric distance, the interstellar mass is about equally distributed in diffuse and molecular cloud components, and so grain material spends as much time in each. Thus the evolution of grains as the medium passes from molecular to a more diffuse cloud state is just as important. As distinct from these more dramatic intracycle changes, the effects of some physical processes might be slower yet cumulative over many cycles, causing a secular change in the size distribution; what we observe must then be considered also as the end product of many cycles.

Among the processes to be considered are coagulation (Chokshi, Tielens, & Hollenbach 1993), fragmentation in grain-grain collisions and sputtering in shock waves (Biermann & Harwit 1980; Seab & Shull 1983; McKee et al. 1987), accretion of atoms and molecules (Draine 1990; Tielens 1989), and erosion and photoprocessing of accreted mantles (Jenniskens et al. 1993). Presumably different mechanisms would dominate in different environments and on different timescales (with secular effects or not). Whether a steady state size distribution is obtained in either phase depends on the timescales for various grain alteration processes compared to the cycling time. The variety of values of R_V found in dark clouds as opposed to the more uniform $R_V = 3.1$ of the diffuse cloud medium suggests that timescales are important, and that there might be differences in size distributions related to the direction of evolution. Identification of systematic environmental changes and deviations from the average extinction curves for a given R_V must provide additional important empirical clues to the evolutionary processes (Clayton & Cardelli 1988; Cardelli & Clayton 1991; Mathis & Cardelli 1992; Jenniskens & Greenberg 1993). A comprehensive treatment of the entire evolution is beyond the scope of this paper, but is certainly an important goal (Liffman & Clayton 1989).

Mathis (1989) has argued that the case for a power-law size distribution with a slope like that measured in diffuse clouds is strong. From a theoretical standpoint, shattering of grains could establish such a power law, at least over the range of sizes in which there is a steady state (Biermann & Harwit 1980; Dorschner 1982; Hayakawa & Hayakawa 1988). Observationally, power-law size distributions are found in many diverse circumstances: in the rings of Saturn (Cuzzi et al. 1984), in meteoroids (Napier & Dodd 1974), and in various kinds of terrestrial and lunar rocky and sandy debris (Hartmann 1969). It is sobering, however, that the direct evidence from extinction pointing to a power law exists only over 1 decade in grain size.

In the derived size distributions we find many more small particles in the diffuse cloud case. Thus, shattering might be implicated if there are many grain-grain collisions during disruption of the molecular cloud phase by supernova shocks, winds from massive stars, and bipolar outflows. The uniformity of R_V in the diffuse clouds might suggest that most of the shattering evolution occurs rapidly during disruption of

the molecular clouds, and that further evolution of the size distribution by other processes during the diffuse cloud stage is limited. This needs to be quantified. It is also probably significant that the power law is of the slope observed, having much of the mass remaining at the large particle end; production of such a power law is fairly stable and could reach a relatively uniform steady state.

Shattering might not be the sole disruptive process, however. The decrease in gas phase depletion in high-velocity diffuse material is suggestive of complete vaporization or sputtering (Seab 1987); since these processes must occur to some degree in the hot gas in supernova shocks, and shocks accelerate gas, this is a persuasive portion of the evolutionary picture. As well as the disruption of grains emerging from the molecular cloud phase, we would include erosion of the diffuse cloud grains too.

Chokshi et al. (1993) have recently examined the reverse physical process, coagulation, in some detail. They conclude that coagulation of large particles ($a > 0.1$ μm) does not proceed very efficiently in dense clouds, although it is enhanced when grains are covered with ice mantles; a doubling of size within a dense cloud lifetime might be possible. By contrast, relative velocities acquired by small grains in a turbulent medium are smaller and so small grains do tend to stick to one another and to the larger grains on the available timescale. Given the slope of the "initial" (diffuse cloud) size distribution, this can cause major changes in the small particle end of the size distribution, yet only mild growth at the larger particle end. Such an alteration of the size distribution is what was inferred empirically by Martin & Whittet (1990) based on the relative "universality" of the infrared extinction and polarization curves despite extensive changes in the optical and the ultraviolet. The derived MEM size distributions are in agreement with this picture too, putting it on a more quantitative basis. Attributing these changes to accretion seems unlikely to us (see below). Although coagulation seems attractive and viable, there are many interesting detailed issues to address (is there evidence from the MEM size distributions that small graphite particles are somewhat less susceptible to coagulation and can this be understood; are composite grains produced in dense clouds; how does shattering of composite grains differ from shattering of solid grains; do composite grains survive passage into the diffuse cloud medium; why does the size distribution have a cutoff for particles bigger than ~ 0.2 μm?).

Coagulation and shattering (if not reaching vaporization) merely redistribute mass and it has been argued that these are the major processes responsible for the intra-cycle changes of the size distribution. Let us finally consider the secular buildup of grains. Historically accretion has been very prominent theoretically. Oort & van de Hulst (1946) derived a size distribution of interstellar grains by postulating steady state growth and destruction, where destruction probablility is proportional to the grain area. They noted that the size distribution was not unique; there might be various other forms giving similar optical extinction curves (ultraviolet extinction and interstellar polarization were as yet unknown). By introducing a simple area-dependent destruction process Greenberg (1968) derived a size distribution of the form $\exp(-\alpha a^3)$, which closely approximated the Oort–van de Hulst distribution. Assuming that the optical extinction and polarization are caused by the same grains, Hong & Greenberg (1978) showed that among a variety of single parameter size distributions, this function best yields the most commonly observed combination $R_V \simeq 3$ and $\lambda_{max} \simeq 0.545$ μm (the wavelength where polarization reaches maximum). However, we note that adherence to this form of size distribution predicts that λ_{max} decreases when R_V increases, contrary to what is observed. Nor does this model address the ultraviolet extinction. These models in which grains are grown largely by accretion are probably now irrelevant.

Nevertheless, accretion must be of some secular importance. For example, Jura (1987) has pointed out that in the absence of a depletion process in the interstellar medium, admixture of grain free stellar winds from hot stars would result in unacceptable gas phase abundances of species such as Fe which are observed to be highly depleted. There could be a similar problem for Si from carbon stars (Martin & Rogers 1987). Furthermore, repeated estimates of grain destruction rates by shocks (Seab 1987; McKee 1989) find grain lifetimes which are short compared to the injection time of new material into the interstellar medium, which again demand efficient accretion to avoid discordantly high gas phase abundances of what are observed to be depleted species. Draine (1990) showed that the accretion of Si onto dust would be strongly suppressed in diffuse clouds and the timescale for any accretion is in any case long. On the other hand, accretion occurs more efficiently with increasing density, and indeed spectral features of ice mantles are detected in sufficiently dense clouds. However, the implied mass of material in the ice mantles is quite small ($\sim 10\%$ of the mass of grains already present; Jenniskens et al. 1993). This is perhaps not surprising, since the depletion *in the present day interstellar medium* is already high in the diffuse cloud material from which molecular clouds assemble. The ice mantles distributed over large grains are correspondingly thin (0.02 μm) and so do not account for the inferred changes in the size distribution in dense clouds.

It has been proposed that ultraviolet processing during the molecular cloud phase will alter the ices, leaving a more refractory organic residue which can more readily survive the return to the diffuse interstellar medium (Jenniskens et al. 1993 and references therein). It is argued further that in the unshielded diffuse medium, further processing could drive off the H, N, and O, carbonizing and even polymerize the material. Depending on the yield per cycle, this could be a much more important source of new carbon grains than injected by carbon-rich AGB stars: while the fraction of material being processed in this way might be small at any one time, over many cycles through the molecular clouds the total amount of such material could accumulate. One spectral feature to support this scenario is the 3.4 μm absorption feature attributed to C-H stretching vibrations. This feature is present for several Galactic center sources and for the heavily reddened star Cyg OB2 no. 12 (Adamson, Whittet, & Duley 1990 and references therein). The most persuasive evidence is the detection of subpeaks near 2955, 2925, and 2870 cm^{-1} by Sandford et al. (1991). These features are attributed to C-H stretching vibrations in the $-CH_2-$ and $-CH_3$ groups of aliphatic hydrocarbons. They conclude from the relative strengths of these subpeaks that short chain organic materials are present in the diffuse interstellar medium. We can make an indirect argument as well in support of this, using observations of the O/H ratio. The solar abundance of O/H is 8.5×10^{-4} (Grevesse & Anders 1989), and yet the gas phase O I/H is only 3×10^{-4} (Cardelli et al. 1993) and silicates use at most 4Si/H or 1.3×10^{-4}. Therefore, unless the solar O/H is unrepresentatively high, about half of the O/H is unaccounted for. If the O/C ratio in the organic residue were still substantial, and the residue (rather than graphite) were a major sink for C, this would work in the direction of explaining the missing O/H.

There would be several interesting consequences of this

model. An obvious one would be that the basic building blocks we used, bare graphite and silicate, are not entirely appropriate. Instead it is imagined that the silicate material is in the form of grain cores with rather thick mantles of the residue. Given the dielectric function (Jenniskens 1993), it should be possible to incorporate such a material into the MEM solutions, in the form of core-mantle particles or even simple homogeneous particles. The latter could arise if substantial shattering of the mantle material occurs during grain cycling; ultimate products could also include small graphitic grains and PAHs. The core-mantle structure also has another potentially interesting implication for grain processing: the silicate material might be protected and have a higher survival rate against shock destruction (e.g., Liffman & Clayton 1989). This is an important consideration since the silicate injection rate from stars is probably comparable to that of carbon grains, and there is no proposed interstellar source for silicate; it would also help keep the Si in pure silicate form. If the silicate cores are not shattered, then there might not be any small silicate grains (which would remain bare because of temperature fluctuations); and, as discussed in § 5.2, there would be no nonequilibrium emission at the 10 μm feature.

7. SUMMARY

The size distribution of interstellar dust particles has been determined by fitting the parameterized CCM extinction curve for $R_V = 3.1$ and for $R_V = 5.3$. A bare graphite-silicate model was used, as underlies MRN. The results obtained from MEM analysis are as follows.

1. For the case of $R_V = 3.1$, our MEM size distributions resemble a power law with an exponential cutoff, roughly similar in slope to the MRN power law within the range from rather small to intermediate sizes (0.02–0.2 μm). Despite the overall similarity to MRN, there are important differences in the MEM size distributions. At intermediate sizes (0.02–0.2 μm), the MEM size distributions have more structure than a simple power law. This structure is robust within the context of this graphite-silicate model and is necessary to achieve a good fit to the detailed optical and near-ultraviolet extinction. The sharp cutoff in the MRN distribution at a_+ is clearly unphysical and is of concern since $m(a)a$ is still rising. Our MEM result shows a smooth decrease beginning at ~ 0.2 μm; this decrease out to ~ 1.0 μm is forced on the solution by the extinction data. We also fitted parameterized PED size distributions to the extinction data for an independent check of results. The power-law slope for silicate is -3.06 and for graphite is -3.48 and the values of a_b are 0.14 μm for silicate and 0.28 μm for graphite (a_- was set to 0.0025 μm). The intention of this work is not to specify a_+ and a_-: a_+ is not relevant since there is a turndown in the size distribution (a_b); there simply is not enough information within the available wavelength range (from 0.1 to 5.1 μm) for particles smaller than 0.02 μm and for particles larger than 1.0 μm.

2. The amounts of C and Si consumed in grains are comparable to those of the MRN model ($R_V = 3.1$): 3.37×10^{-5} Si atoms per H or 95% of the adopted cosmic abundance is required to be in silicates; the graphite component uses 3.0×10^{-4} C atoms per H.

3. To minimize the graphite requirement, amorphous carbon was added to the graphite-silicate model. The overall size distributions for two- and three-composition models are similar. But the detailed structure is not the same, and thus one must be cautious in interpreting it; the MEM size distribution will be a good solution for the adopted building blocks.

4. From the MEM size distributions we calculated the albedo and the asymmetry parameter of the phase function of the interstellar grains. Within the wavelength range 0.01–1.0 μm the values for $R_V = 3.1$ are quite similar to those of MRN. However, the MRN and our MEM size distributions are different for particles larger than 0.2 μm, and so there are significant differences in the infrared (>1 μm). Compared to the MRN model, the scattering is somewhat less isotropic, but the more important difference is in the albedo, which is markedly increased toward longer wavelengths.

5. The size distribution for $R_V = 5.3$ is different from that of $R_V = 3.1$. By construction, the total mass in this model is about the same as for $R_V = 3.1$. But, there is a great reduction in the relative numbers of particles with a <0.1 μm, and some increase for larger particles. This now quantifies our understanding of the origin of the change of the shape of the optical extinction curve (R_V) and the reduction in the ultraviolet extinction.

Added note: Further analysis of the far-ultraviolet albedo by Witt et al. (1993) and Murthy et al. (1993) are in improved agreement with our model.

This work was supported by the Natural Sciences and Engineering Research Council of Canada.

REFERENCES

Adamson, A. J., Whittet, D. C. B., & Duley, W. W. 1990, MNRAS, 243, 400
Biermann, P., & Harwit, M. 1980, ApJ, 241, L105
Bohlin, R. C., Savage, B. D., & Drake, J. F. 1978, ApJ, 224, 132
Boroson, T. A., & Witt, A. N. 1990, ApJ, 355, 182
Boulanger, F., Falgarone, E., Helou, G., & Puget, J.-L. 1989, in Interstellar Dust: Contributed Papers, ed. A. G. G. M. Tielens & L. J. Allamandola (NASA CP 336), 123
Cardelli, J. A., & Clayton, G. C. 1991, AJ, 101, 1021
Cardelli, J. A., Clayton, G. C., & Mathis, J. S. 1989, ApJ, 345, 245 (CCM)
Cardelli, J. A., Mathis, J. S., Ebbets, D. C., & Savage, B. D. 1993, ApJ, 402, L17
Chokshi, A., Tielens, A. G. G. M., & Hollenbach, D. 1993, ApJ, 407, 806
Clayton, G. C., & Cardelli, J. A. 1988, ApJ, 327, 911
Cuzzi, J. N., Lissauer, J. J., Esposito, L. W., Holberg, J. B., Marouf, E. A., Tyler, G. L., & Boischot, A. 1984, in Planetary Rings, ed. R. G. Greenberg & A. Brahic (Tucson: Univ. of Arizona Press), 73
Désert, F.-X., Boulanger, F., Léger, J. L., Puget, J. L., & Sellgren, K. 1986, A&A, 159, 328
Désert, F.-X., Boulanger, F., & Puget, J. L. 1990, A&A, 237, 215
Dorschner, J. 1982, Ap&SS, 81, 323
Draine, B. T. 1985, ApJS, 57, 587
———. 1988, ApJ, 333, 848
Draine, B. T. 1990, in The Evolution of the Interstellar Medium, ed. L. Blitz (San Francisco: ASP), 193
Draine, B. T., & Anderson, N. 1985, ApJ, 292, 494
Draine, B. T., & Lee, H.-M. 1984, ApJ, 285, 89
Greenberg, J. M. 1968, in Nebulae and Interstellar Matter, ed. B. M. Middlehurst & L. H. Aller (Univ. of Chicago Press), 221
Grevesse, N., & Anders, E. 1989, AIP Conf. Proc. 183, ed. R. G. Lerner (New York: AIP), 1
Hartmann, W. K. 1969, Icarus, 10, 201
Hayakawa, H., & Hayakawa, S. 1988, PASJ, 40, 341
Hendry, P. D. 1994, in preparation
Hong, S. S., & Greenberg, J. M. 1978, A&A, 70, 695
Hurwitz, M., Bowyer, S., & Martin, C. 1991, ApJ, 372, 167
Jenniskens, P. 1993, A&A, 274, 653
Jenniskens, P., Baratta, G. A., Kouchi, A., de Groot, M. S., Greenberg, J. M., & Strazzula, G. 1993, A&A, 273, 583
Jenniskens, P., & Greenberg, J. M. 1993, A&A, 274, 439
Jura, M. 1987, in Interstellar Processes, ed. D. J. Hollenbach & H. A. Thronson (Dordrecht: Reidel), 3
Laureijs, R. J., Mattila, K., & Schnur, G. 1987, A&A, 184, 269
Liffman, K., & Clayton, D. D. 1989, ApJ, 340, 853

Lillie, C. F., & Witt, A. N. 1976, ApJ, 208, 64
Martin, P. G., & Rogers, C. 1987, ApJ, 322, 374
Martin, P. G., & Whittet, D. C. B. 1990, ApJ, 357, 113
Mathis, J. S. 1979, ApJ, 232, 747
———. 1989, in IAU Symp. 135, Interstellar Dust, ed. L. J. Allamandola & A. G. G. M. Tielens (Dordrecht: Kluwer), 357
———. 1994, ApJ, 422, 176
Mathis, J. S., & Cardelli, J. A. 1992, ApJ, 398, 610
Mathis, J. S., Rumpl, W., & Nordsieck, K. H. 1977, ApJ, 217, 425 (MRN)
Mathis, J. S., & Wallenhorst, S. G. 1981, ApJ, 244, 483
Mathis, J. S., & Whiffen, G. 1989, ApJ, 341, 808
McKee, C. F. 1989, in IAU Symposium 135, Interstellar Dust, ed. L. J. Allamandola & A. G. G. M. Tielens (Dordrecht: Kluwer), 431
McKee, C. F., Hollenbach, D. J., Seab, C. G., & Tielens, A. G. G. M. 1987, ApJ, 318, 674
Meyer, J.-P. 1988, in Origin and Distribution of the Elements, ed. G. J. Mathews (Singapore: World Scientific), 337
Morgan, D. H. 1980, MNRAS, 190, 825
Murthy, J., Dring, A., Henry, R. C., Kurk, J. W., Blair, W. P., Kimble, R. A., & Durrance, S. T. 1993, ApJ, 408, 197
Napier, W. McDD., & Dodd, R. J. 1974, MNRAS, 166, 469
Onaka, T., & Kodaira, K. 1992, ApJ, 379, 532
Oort, J. H., & van de Hulst, H. C. 1946, Bull. Astron. Inst. Netherlands, 10, 187
Pendleton, Y. J., Tielens, A. G. G. M., & Werner, M. W. 1990, ApJ, 349, 107
Rouleau, F., & Martin, P. G. 1990, ApJ, 377, 526
Rowan-Robinson, M. 1992, MNRAS, 258, 787
Seab, C. G. 1987, in Interstellar Processes, ed. D. J. Hollenbach & H. A. Thronson (Dordrecht: Reidel), 491
Seab, C. G., & Shull, J. M. 1983, ApJ, 275, 652
Sellgren, K., Allamandola, L. J., Bregman, J. D., & Wooden, D. H. 1985, ApJ, 299, 416
Sellgren, K., Luan, L., & Werner, M. W. 1990, ApJ, 359, 384
Sellgren, K., Werner, M. W., & Dinerstein, H. L. 1992, ApJ, 400, 238
Siebenmorgen, R., Krügel, E., & Mathis, J. S. 1992, ApJ, 266, 501
Skilling, J. 1981, Algorithms and Applications, presented at Workshop on Maximum Entropy, Laramie, Wyoming
Tielens, A. G. G. M. 1989, in Interstellar Dust, ed. L. J. Allamandola & A. G. G. M. Tielens (Dordrecht: Kluwer), 239
Witt, A. N., Petersohn, J. K., Bohlin, R. C., O'Connell, R. W., Roberts, M. S., Smith, A. M., & Stecher, T. P. 1992, ApJ, 395, L5
Witt, A. N., Petersohn, J. K., Holberg, J. B., Murthy, J., Dring, A., & Henry, R. C. 1993, ApJ, 410, 714